Fluid Dynamics & Materials Processing

Tech Science Press

DOI: 10.32604/fdmp.2021.015612

ARTICLE

Preparation and Characterization of Electrospun Polylactic Acid Micro/Nanofibers under Different Solvent Conditions

Hao Dou[1,2,*], Hongxia Liu[1,2], Feng Wang[1,2] and Yanli Sun[1,2]

[1]School of Textile Science and Engineering, Xi'an Polytechnic University, Xi'an, 710048, China

[2]State Key Laboratory of Intelligent Textile Material and Products, Xi'an Polytechnic University, Xi'an, 710048, China

[*]Corresponding Author: Hao Dou. Email: douhaosuda@126.com

Received: 31 December 2020 Accepted: 01 March 2021

ABSTRACT

Electrospinning is a versatile and popular method for the fabrication of ultrafine fibers and many parameters in electrospinning can be adjusted when ideal micro/nanofibers are required. In particular, the selection of a proper solvent condition is a fundamental and crucial step to produce electrospun ultrafine fibers. In this study, a commonly used biomaterial, polylactic acid (PLA), was dissolved in 7 different solvents and PLA micro/nanofibers were prepared by electrospinning. The morphology, porosity, mechanical property and static contact angle were characterized to determine the quality of the obtained product. The results show that different solvent conditions have a significant effect on both the diameter, surface smooth degree of PLA micro/nanofibers and the properties of the fibrous membranes.

KEYWORDS

PLA; micro/nanofibers; solvent conditions; electrospinning

1 Introduction

Fibers are continuously solid state but soft materials, which are featured by high flexibility and length to diameter ratio [1]. Ultrafine fibers are usually defined as fibrous structures with diameters around or below the micro-scale range. Due to the intrinsic properties such as tiny diameter, high specific surface area and small pore size with high porosity, ultrafine fibers especially nanofibers have been widely used in diverse fields including filtration and separation, drug delivery and tissue engineering, energy and electronics, etc. [2–4].

Electrospinning, including a simple and favorable method called bubble electrospinning for the mass-production of nanomaterials [5], has attracted many interests in the fabrication of micro/nanofibers because of its advantages in processing various materials and its ease in operation as well as its low cost in the manufacture setup. As an ideal method of fabricating continuous micro/nanofibers, electrospinning or bubble electrospinning makes use of a high voltage to overcome the surface tension of polymers or polymer bubbles. The electrostatically charged polymer or the ruptured bubble is extremely stretched into micro/nanofibers under high electric field force. Finally, the resulting micro/nanofibers are deposited and collected on the grounded electrode with the evaporation of solvent [6–8].

It is well known that there are several factors including polymer properties, processing parameters and environmental conditions [9], having critical effects on the micro-structure and properties of electrospun

micro/nanofibers in the electrospinning process. In particular, choices of solvents for polymer dissolution have a crucial influence on the properties of electrospinning solutions, which determine the spinnability, morphology of products like the fiber diameter and structure, the relationship between fibers, the porosity, and mechanical properties of micro/nanofibrous membranes [10,11]. For example, Wannatong et al. [12] used six solvents with different properties for the preparation of electrospun polystyrene fibers and reported that polystyrene fiber diameter decreases with increasing solvent boiling point. Guerrini et al. [13] evaluated the influence of different solvents or mixtures on the morphology of pullulan nanofibers and found solvents and solvent mixtures were closely related to the morphology and diameters of the nanofibers. In addition, Peng et al. [14] developed a Richford-Rice like equation and discussed the influence of rapid solvent evaporation on the fiber morphology in the bubble electrospinning, which provided a theoretical model for multi-solvent solutions.

Recently, there is a growing focus on the research of PLA which is one of the most promising biomaterials and PLA has been regarded as the most commercially available and biodegradable thermoplastic polymer [15,16]. Because PLA has been officially approved by the Food and Drug Administration (FDA), PLA micro/nanofibers has been extensively used for the drug delivery, wound dressings and tissue scaffold [17–19]. However, the intrinsic brittleness, hydrophobic surfaces, acidic degradation of PLA micro/nanofibers induces poor mechanical properties which limits its use in lots of aspects. Hence, it is absolutely necessary to enhance the mechanical performance of PLA micro/nanofibers to meet practical and desired requirements [20–23]. Several scientific papers [24–26] have indicated that PLA can be well dissolved in some organic solvents like dichoromethane (DCM), chloroform (CF), acetone, N,N-Dimethylformamide (DMF) and Dimethylacetamide (DMA). For example, Liu et al. [27] used a binary solvent of DCM with high vapor pressure and DMA with low vapor pressure for the fabrication of electrospun PLA porous nanofibers and found phase separation occurred due to solvent evaporation, leading to different fiber diameters and pore sizes. So it is a good strategy to change the solvents or ratios of solvent mixtures to obtain different micro-structures and properties of micro/nanofibrous membrances, as properties of spinning solutions which play a key impact on the electrospinning are strongly dependant on the type of solvents.

In this paper, DCM, CF and DMF were selected and mixed to prepare different spinning solutions. In addition, the influence of solvent choice on PLA micro/nanofibers' morphology and properties were investigated.

2 Materials and Methods

2.1 Materials

PLA (Type: 4032D) was purchased from NatureWorks, USA. DCM and CF were purchased from Tianjin Damao Chemical reagent factory, China. DMF and ethanol were purchased from Tianjin Kaitong Chemical reagent factory, China. Calcium chloride ($CaCl_2$) was purchased from Tianjin Zhiyuan Chemical reagent factory, China. All raw materials were AR grade and used as received. PLA was vacuum dried before use.

2.2 Preparation of the PLA Micro/Nanofibrous Membranes

In order to investigate the effect of different solvents on the spinnability, morphology and properties of PLA micro/nanofibers, 6% PLA solutions were dissolved in seven different solvents or solvent mixtures, respectively. Besides, it is reported that the addition of inorganic salts will be in favor of electrospinning process and can effectively eliminate the beaded fibers due to increasing the conductivity of polymer solutions [28], so $CaCl_2$ was added in S7 compared with S6 to study whether the morphology and properties of obtained outcome change. The specific formulation of the electrospinning solutions in this paper was listed in Tab. 1. Each solution was stirred for 4 h at room temperature to form the final

well-dissolved solution. Then, the corresponding solution was fed into a 10 mL plastic syringe controlled by a syringe pump at a feeding rate of 0.5–1.0 ml/h. The needle was subjected to a high-voltage DC power of 15 kV and the collector for the deposition of resultant fibers was positioned 15 cm away from the needle tip. All experiments were carried out for 6 h in a chamber with relative humidity (RH) 50% at room temperature. Further, the micro/nanofibrous membranes were vacuum dried for 12 h to remove any residual solvent. Finally, all samples with different solvent parameters were labeled as shown in Tab. 1, respectively.

Table 1: The sample formulation of spinning solutions with different solvent parameters

Sample number	Solution concentration	Percentage of different solvents				
		CF	DCM	DMF	Ethanol	$CaCl_2$
S1	6% PLA	100%				
S2	6% PLA	90%		10%		
S3	6% PLA	80%		20%		
S4	6% PLA		100%			
S5	6% PLA		90%	10%		
S6	6% PLA		90%		10%	
S7	6% PLA		85.7%		9.5%	4.8%

2.3 Characterization and Measurements

All samples from the electrospun micro/nanofibers were mounted on a copper plate and sputter-coated (X-MAX50, Oxford, UK) for 90 s with a gold layer 20–30 nm thick prior to imaging (Quanta-450-FEG, Oxford, UK). The morphology was observed using a scanning electron microscopy (SEM) at 20°C, 60% RH. In order to display the diameter distribution and the average diameters, the micro/nanofibers were measured from randomly collected SEM images by means of the ImageJ software and expressed as mean ± standard deviation (SD).

The micro/nanofibrous membranes (50 mm × 10 mm) were put before all tests in standard conditions (20 ± 2°C, RH 65 ± 5%) for 24 h, and then measured on a mechanical testing instrument (Instron 3365, USA) equipped with a 2 cN load at a 10 mm/min stretching speed. The clamping length was 20 mm. The results were the average tensile data from at least five specimens. The breaking stress and breaking elongation of all samples were calculated according to the following equations:

$$\text{The breaking stress(MPa)} = \frac{\text{the breaking strengh (N)}}{\text{membrane thickness (mm)} \times \text{membrane width (mm)}} \tag{1}$$

$$\text{The breaking elongation(\%)} = \frac{\text{the breaking length (mm)}}{\text{the clamping length(mm)}} \times 100\% \tag{2}$$

The micro/nanofibrous membranes were cut into 20 mm × 20 mm samples, and then the thickness of the membranes was tested with a micrometer on five different points of membranes. Finally, each sample of membranes was weighed on the electronic balance and the average weight was taken from three groups of each sample. The porosity of micro/nanofibrous membranes was calculated according to the following equations:

$$\varepsilon = 1 - \frac{\rho}{\rho_0} \tag{3}$$

$$\rho = \frac{\mathrm{m}}{d \times S} \tag{4}$$

where ε is the porosity of micro/nanofibrous membranes, ρ_0 is the density of PLA raw material, ρ, m, d, S is the density, the mass, the thickness and the surface area of micro/nanofibrous membranes, respectively.

The contact angle was obtained from the Contact Angle Analyzer (OCA-40, DataPhysics, Germany). Pure distilled water with 5 μL volume was dropped on the membrane surface (10 mm × 10 mm). The determination of all contact angles was finished within 5 s after each drop to ensure that the droplet did not soak into the sample. The final contact angles used were based on the mean of 3 determinations.

3 Results and Discussions

3.1 Morphological Analysis of Electrospun PLA Micro/Nanofibers

Fig. 1 shows the images of the SEM morphology and diameter statistics of the electrospun PLA micro/nanofibers. It can be seen from Fig. 1 that the micro/nanofibers in each sample has different degrees of adhesion with the dendritic structure, which will be in favor of increasing the stress of the fibrous membranes. Based on the result of data statistics, the average fiber diameters of S1, S2, S3, S4, S5, S6 and S7 are 2062 ± 843 nm, 1178 ± 424 nm, 809 ± 309 nm, 4308 ± 1406 nm, 948 ± 422 nm, 623 ± 251 nm and 883 ± 319 nm, respectively. This is an interesting phenomenon indicating that the fiber diameter can be adjusted by changing the type and mixture ratio of solvents. Furthermore, the diameter comparison among S1, S2 and S3 shows that with the decrease of the DCM component, the tightness between fibers increases while the diameter of fibers decreases and the diameter distribution becomes narrow. On the other hand, dramatic drop of the fiber diameter from S4 to S5 is observed. With the reduction of CF content, the fiber diameter decreases sharply but the degree of adhesion between fibers rises rapidly. When ethanol was added into the solvent in S6 sample, the spindles which form the cross-over points between fibers like liquid drops obviously appear on the surface of micro/nanofibers. The reason for this special structure may be that the moisture in the air inhibits the evaporation of ethanol under the condition of 50% RH, which leaves part ethanol exist in the form of liquid state when final fibers arrive on the collector, and results in the inadequate stretch [29] and the formation of adhesion. However, the spindle structure disappears in S7 which contains 4.8% $CaCl_2$, but the situation of the adhesion between fibers still exists. This can be attributed to the conductivity improvement of the spinning solution in the presence of calcium ions, which will be benefit to the spinnability and ultrafine fibers' formation.

3.2 Porosity Analysis of PLA Micro/Nanofibrous Membranes

The porosity of micro/nanofibrous membranes refers to the ratio of the pore volume to the total volume of micro/nanofibrous membranes, which can reflect the permeability and gas exchange ability. One of advantages of ultrafine fibers obtained by electrospinning is the high porosity. Tab. 2 shows the porosity of electrospun PLA micro/nanofibrous membranes. It can be seen from Tab. 2 that the porosity of the fibrous membranes has a great relationship with the surface morphology and the diameter of the micro/nanofibers. The overall trend is that the smoother the surface structure of micro/nanofibers with bigger diameter, the less the porosity of micro/nanofibrous membranes. Except for S6 with 68.21% porosity, the porosity of other samples is above 80% due to the high and fast evaporation of CF and DCM. On the other side, ethanol was added in both S6 and S7. When the RH is 50%, the volatilization of ethanol is limited, which leads to more adhesion between fibers and causes side-by-side fibers, resulting in the decrease of porosity of S6. But S7 contains calcium ions, which can improve the conductivity and spinnability during the electrospinning process and lessen the irregular structure like spindles on the surface of micro/nanofibers. The results show that the dissolution of PLA with different solvents has a significant influence on the internal structure of micro/nanofibrous membranes, which causes the different porosity.

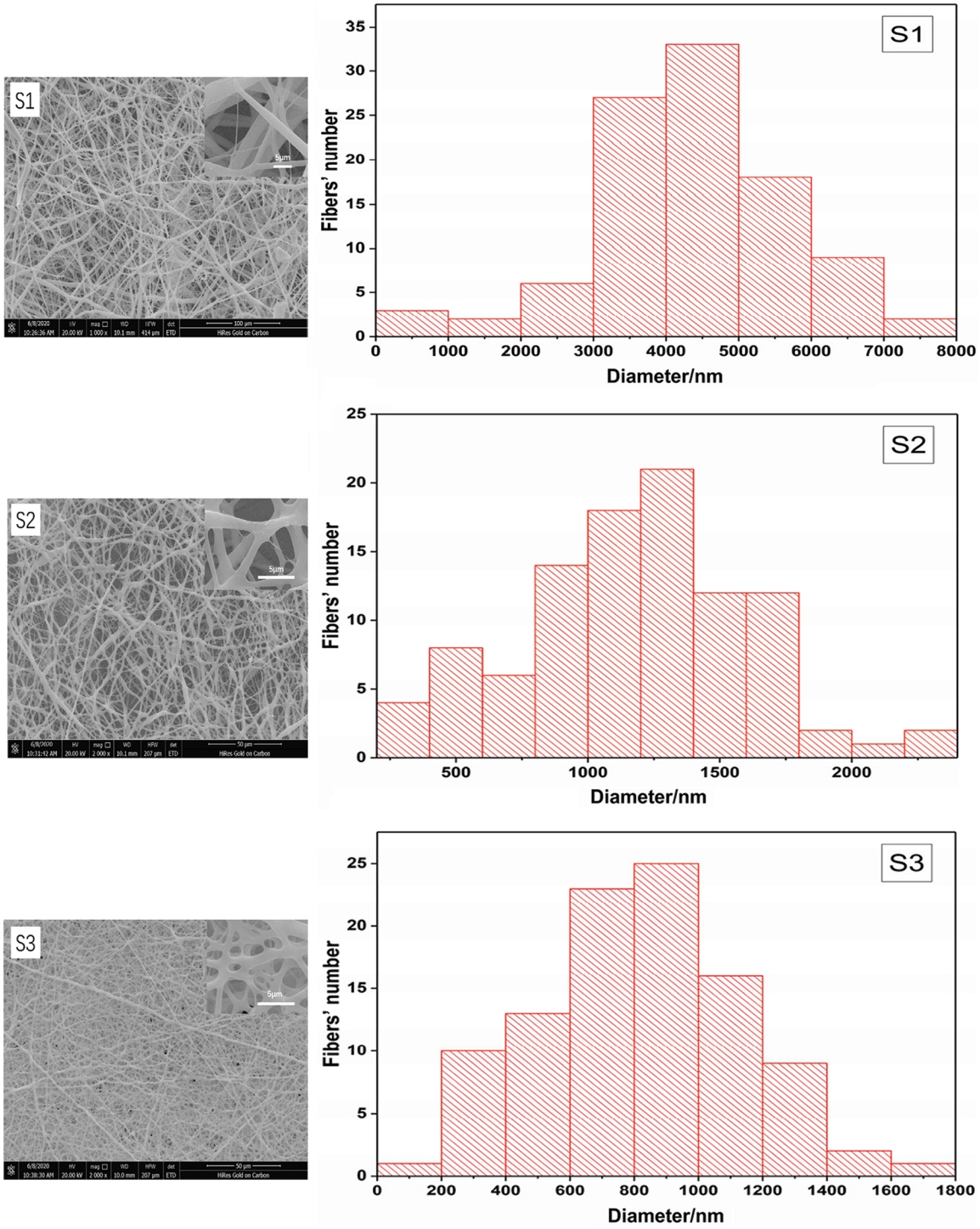

Figure 1: (continued)

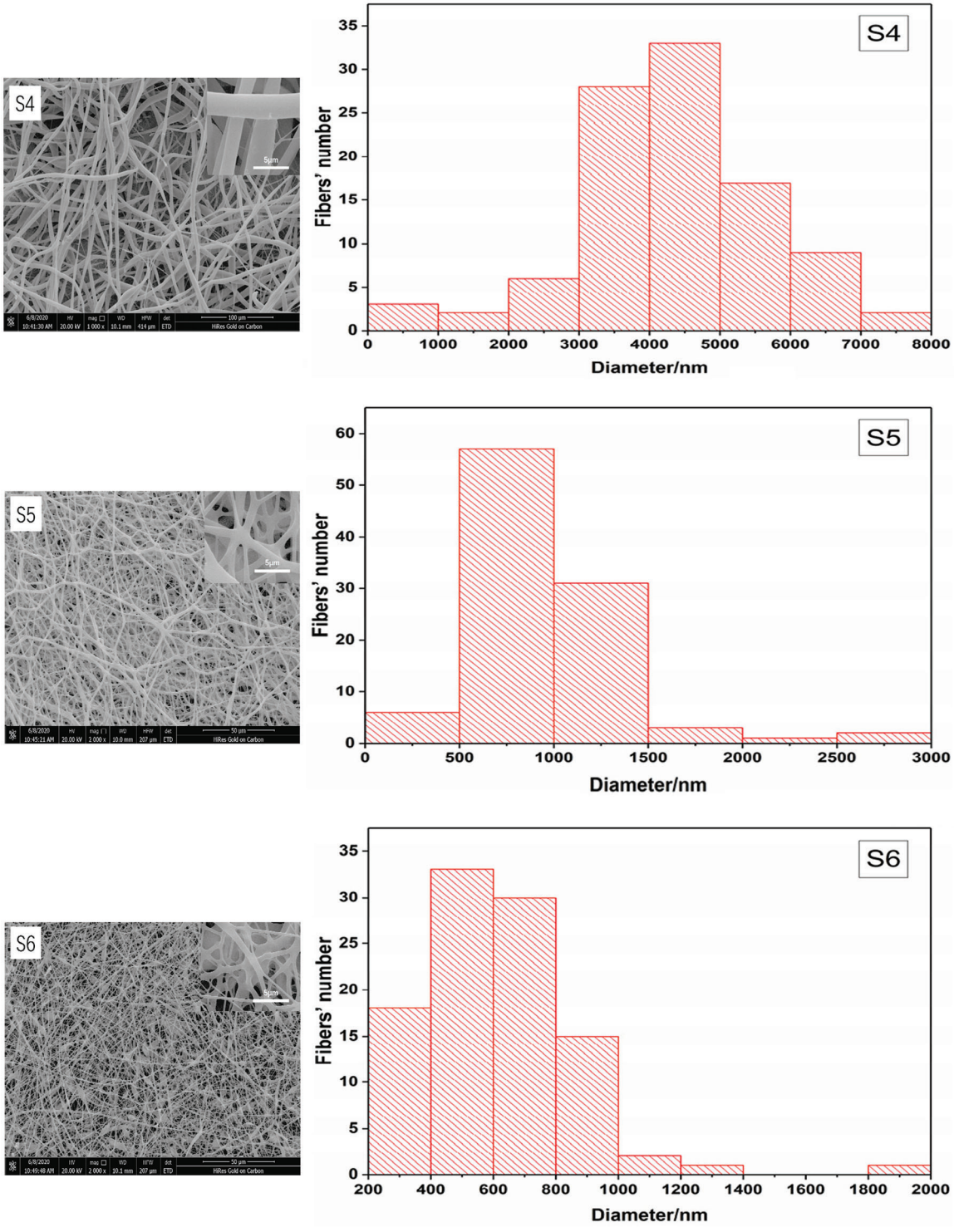

Figure 1: (continued)

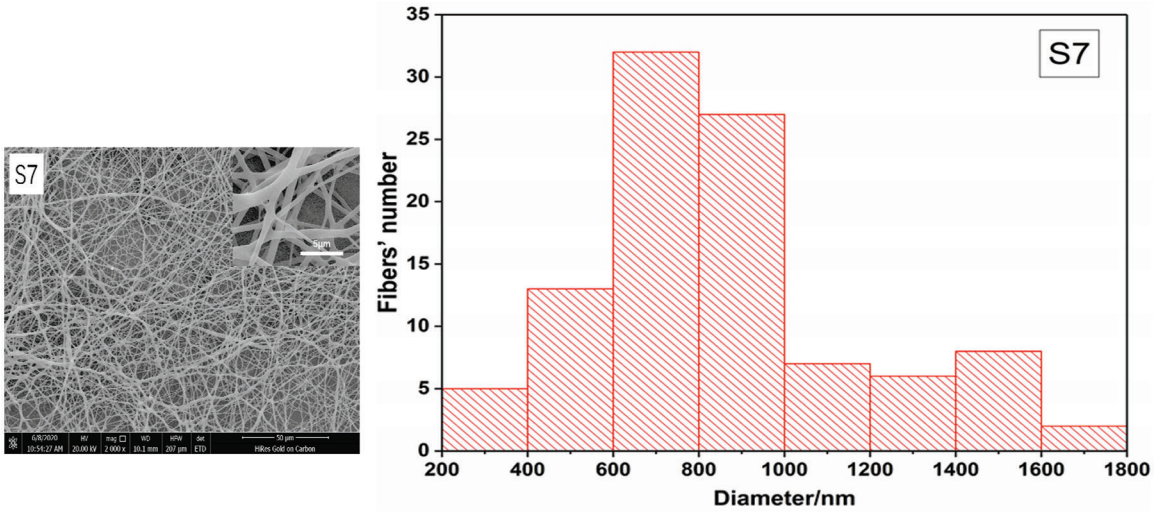

Figure 1: The morphology and diameter statistics of the electrospun PLA micro/nanofibers under different solvent conditions

Table 2: The porosity of the PLA micro/nanofibrous membranes under different solvent conditions

Sample number	ρ(g/cm^3)	ε(%)
S1	0.224	82.11
S2	0.107	91.43
S3	0.195	84.39
S4	0.248	80.14
S5	0.231	81.51
S6	0.397	68.21
S7	0.127	89.82

3.3 Mechanical Property of PLA Micro/Nanofibrous Membranes

The tensile test data of 7 kinds of PLA micro/nanofibrous membranes are shown in Tab. 3. In S1, S2 and S3, with the decrease of the fiber diameter and the diameter distribution, the breaking stress should have increased. However, due to the high porosity and the uneven pore distribution inside the micro/nanofibrous membrane in S2, deformation and weak strength of fibers in the tensile process results in the decrease of the breaking stress. Moreover, the comparison of the breaking stress between S6 and S7, indicates that the spindle structure causes further stretch of charged jets, which increases both the final stress and the breaking elongation.

3.4 Contact Angle of PLA Micro/Nanofibrous Membranes

The contact angle is used to assess the surface wettability of materials. If the water droplets on the material surface have a contact angle of less than 90°, the material is considered hydrophilic. Otherwise, it's hydrophobic. Fig. 2 shows the contact angle of the PLA micro/nanofibrous membranes under seven solvent conditions. Naturally, PLA is a hydrophobic material. So the contact angle of all membranes is greater than 90°, indicating a hydrophobic property. In S1, S2 and S3, the hydrophobicity of the micro/nanofibrous membranes increases first and then decreases. This can be owed to the degree of

fibers' smooth and fineness. But S2 with highest porosity owned the biggest contact angle due to the uneven pore distribution. Besides, S4 and S5 show the same trend to S1 and S3 in the contact angle, namely the contact angle decreases when the fiber diameter decreases. In S6, the contact angle is least, which is related to the water conductivity of the spindle structure and the ethanol used. Fan et al. [30] thought that the boundary-induced forces by adjacent nanofibers are randomly directed for a randomly distributed nanofiber membrane. This is due to the the geometric potential theory. Yao et al. [31] found it is the pressure difference pushing the particles and solvents from the centre to the boundary of charged moving jets, leading to the formation of non-smooth surface of micro/nanofibers with high surface energy (geometric potential). So the different shapes of micro/nanofibers generated by different solvent evaporation bring about different contact angles.

Table 3: The tensile data of PLA micro/nanofibrous membranes under different solvent conditions

Sample number	The breaking elongation/%	The breaking stress/MPa
S1	34.61 ± 0.57	1.31 ± 0.34
S2	32.60 ± 0.42	0.64 ± 0.22
S3	48.98 ± 1.39	5.28 ± 1.13
S4	16.67 ± 0.27	0.88 ± 0.02
S5	42.30 ± 0.38	1.83 ± 0.16
S6	42.33 ± 0.46	3.21 ± 0.23
S7	35.24 ± 0.51	1.57 ± 0.27

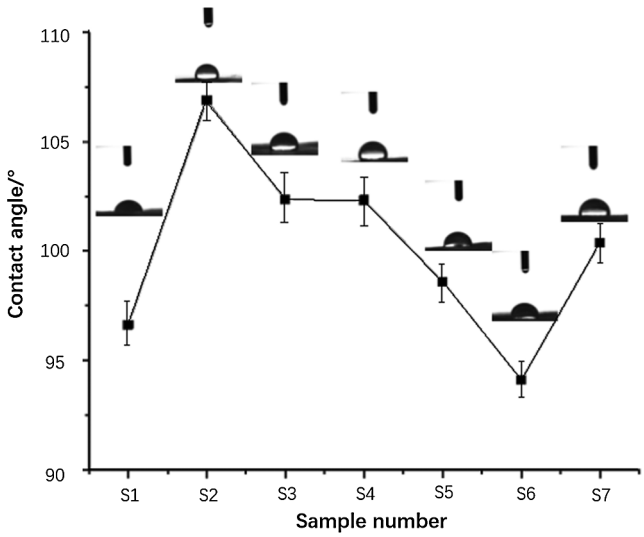

Figure 2: The contact angle of the PLA micro/nanofibrous membranes under different solvent conditions

4 Conclusion

As a parameter affecting properties of the spinning solution, the selection of solvents used in electrospinning is critically important for the formation of micro/nanofibers. The effect of different solvents and solvent mixtures on the morphology and properties of electrospun PLA micro/nanofibers was successfully evaluated. The morphological structure, surface smooth degree of micro/nanofibers can

be effectively controlled by changing the solvent type. Moreover, different solvent conditions also play an essential role in the porosity, the mechanical and wettable property, which will provide a guidance for the choice of PLA micro/nanofibrous membrances for different applications.

Funding Statement: The work is supported by the Doctoral Scientific Research Foundation of Xi'an Polytechnic University (BS15015), Thousand Talents Program of Shaanxi Province, San-qin Scholar Foundation of Shaanxi Province, Scientific Research Program Funded by Shaanxi Provincial Education Department (Program No. 20JK0651) and Priority Academic Program Development of Jiangsu Higher Education Institutions (PAPD).

Conflicts of Interest: The authors declare that they have no conflicts of interests to report regarding the present study.

References

1. Ou, Q. R., Ji, P. J., Xiao, J., Wu, L. (2019). A study on the properties of resin transfer molding cyanate ester and its t800 grade carbon fiber composites. *Fluid Dynamics & Materials Processing, 15(1),* 27–37. DOI 10.32604/fdmp.2019.04787.
2. Bhardwaj, N., Kundu, S. C. (2010). Electrospinning: A fascinating fiber fabrication technique. *Biotechnology Advances, 28(3),* 325–347. DOI 10.1016/j.biotechadv.2010.01.004.
3. Kopp, A., Smeets, R., Gosau, M., Kroger, N., Fuest, S. et al. (2020). Effect of process parameters on additive-free electrospinning of regenerated silk fibroin nonwovens. *Bioactive Materials, 5(2),* 241–252. DOI 10.1016/j.bioactmat.2020.01.010.
4. Beachley, V., Wen, X. J. (2009). Effect of electrospinning parameters on the nanofiber diameter and length. *Materials Science & Engineering: C, 29(3),* 663–668.
5. He, J. H., Kong, H. Y., Yang, R. R., Dou, H., Faraz, N. et al. (2012). Review on fiber morphology obtained by bubble electrospinning and blown bubble spinning. *Thermal Science, 16(5),* 1263–1279. DOI 10.2298/TSCI1205263H.
6. Xue, J. J., Xie, J. W., Liu, W. Y., Xia, Y. N. (2017). Electrospun nanofibers: New concepts, materials, and applications. *Accounts of Chemical Research, 50(8),* 1976–1987. DOI 10.1021/acs.accounts.7b00218.
7. Park, J. H., Kim, M. H., Jeong, L., Cho, D., Kwon, O. H. et al. (2014). Effect of surfactants on sol-gel transition of silk fibroin. *Journal of Sol-Gel Science and Technology, 71(2),* 364–371. DOI 10.1007/s10971-014-3379-4.
8. Jacobs, V., Anandjiwala, R. D., Maaza, M. (2010). The influence of electrospinning parameters on the structural morphology and diameter of electrospun nanofibers. *Journal of Applied Polymer Science, 115(5),* 3130–3136. DOI 10.1002/app.31396.
9. Ilinykh, A. Y. (2020). Spreading of a multicomponent drop in water: Solutions and suspensions. *Fluid Dynamics & Materials Processing, 16(4),* 723–735. DOI 10.32604/fdmp.2020.08987.
10. Yu, M., Dong, R. H., Yan, X., Yu, G. F., You, M. H. et al. (2017). Recent advances in needleless electrospinning of ultrathin fibers: From academia to industrial production. *Macromolecular Materials and Engineering, 302(7),* 1700002. DOI 10.1002/mame.201700002.
11. Mahalingam, S., Raimi-Abraham, B. T., Craig, D. Q. M., Edirisinghe, M. (2015). Solubility-spinnability map and model for the preparation of fibres of polyethylene (terephthalate) using gyration and pressure. *Chemical Engineering Journal, 280,* 344–353. DOI 10.1016/j.cej.2015.05.114.
12. Wannatong, L., Sirivat, A., Supaphol, P. (2004). Effects of solvents on electrospun polymeric fibers: Preliminary study on polystyrene. *Polymer International, 53(11),* 1851–1859.
13. Guerrini, L. M., Oliveira, M. P., Stapait, C. C., Maric, M., Santos, A. M. et al. (2021). Evaluation of different solvents and solubility parameters on the morphology and diameter of electrospun pullulan nanofibers for curcumin entrapment. *Carbohydrate Polymers, 251*. DOI 10.1016/j.carbpol.2020.117127.
14. Peng, N. B., Liu, Y. Q., Xu, L., Si, N., Liu, F. J. et al. (2018). A rachford-rice like equation for solvent evaporation in the bubble electrospinning. *Thermal Science, 22(4),* 1679–1683. DOI 10.2298/TSCI1804679P.

15. Qin, Y. X., Cheng, L. S., Zhang, Y. P., Chen, X. Q., Wang, X. (2018). Efficient preparation of poly (lactic acid) nanofibers by melt differential electrospinning with addition of acetyl tributyl citrate. *Journal of Applied Polymer Science, 135(31),* 46554. DOI 10.1002/app.46554.
16. Koenig, K., Hermanns, S., Ellerkmann, J., Saralidze, K., Langensiepen, F. et al. (2020). The effect of additives and process parameters on the pilot-scale manufacturing of polylactic acid sub-microfibers by melt electrospinning. *Textile Research Journal, 90(17–18),* 1948–1961. DOI 10.1177/0040517520904019.
17. Ghafari, R., Scaffaro, R., Maio, A., Gulino, E. F., Re, G. L. et al. (2019). Processing-structure-property relationships of electrospun PLA-PEO membranes reinforced with enzymatic cellulose nanofibers. *Polymer Testing, 81,* 106182. DOI 10.1016/j.polymertesting.2019.106182.
18. Scaffaro, R., Botta, L., Lopresti, F., Maio, A., Sutera, F. (2017). Polysaccharide nanocrystals as fillers for PLA based nanocomposites. *Cellulose, 24(2),* 447–478. DOI 10.1007/s10570-016-1143-3.
19. Chen, J., Zhang, T. H., Hua, W. K., Li, P. Y., Wang, X. F. (2019). 3D porous poly (lactic acid)/regenerated cellulose composite scaffolds based on electrospun nanofibers for biomineralization. *Colloids and Surfaces A: Physicochemical and Engineering Aspects, 585,* 124048. DOI 10.1016/j.colsurfa.2019.124048.
20. Sharma, D., Satapathy, B. K. (2020). Optimization and physical performance evaluation of electrospun nanofibrous mats of PLA, PCL and their blends. *Journal of Industrial Textiles, 7,* 152808372094450. DOI 10.1177/1528083720944502.
21. Zhu, Z. H., Wu, H. W., Ye, C. L., Wu, W. C. (2017). Enhancement on mechanical and thermal properties of PLA biocomposites due to the addition of hybrid sisal fibers. *Journal of Natural Fibers, 14(6),* 875–886. DOI 10.1080/15440478.2017.1302382.
22. Yin, X. Z., Li, Y., Weng, P. X., Yu, Q., Han, L. et al. (2018). Simultaneous enhancement of toughness, strength and superhydrophilicity of solvent-free microcrystalline cellulose fluids/poly (lactic acid) fibers fabricated via electrospinning approach. *Composites Science and Technology, 167(4),* 190–198. DOI 10.1016/j.compscitech.2018.08.003.
23. Chiesa, E., Dorati, R., Pisani, S., Bruni, G., Rizzi, L. G. et al. (2020). Graphene nanoplatelets for the development of reinforced PLA-PCL electrospun fibers as the next-generation of biomedical mats. *Polymers, 12(6),* 1390. DOI 10.3390/polym12061390.
24. Rogovina, S., Zhorina, L., Gatin, A., Prut, E., Kuznetsova, O. et al. (2020). Biodegradable polylactide-poly (3-hydroxybutyrate) compositions obtained via blending under shear deformations and electrospinning: Characterization and environmental application. *Polymers, 12(5),* 1088. DOI 10.3390/polym12051088.
25. Yang, F., Murugan, R., Wang, S., Ramakrishna, S. (2005). Electrospinning of nano/micro scale poly (l-lactic acid) aligned fibers and their potential in neural tissue engineering. *Biomaterials, 26(15),* 2603–2610. DOI 10.1016/j.biomaterials.2004.06.051.
26. Xu, W. H., Shen, R. Z., Yan, Y. R., Gao, J. (2017). Preparation and characterization of electrospun alginate/PLA nanofibers as tissue engineering material by emulsion eletrospinning. *Journal of the Mechanical Behavior of Biomedical Materials, 65(10),* 428–438. DOI 10.1016/j.jmbbm.2016.09.012.
27. Liu, L. G., He, J. H. (2017). Solvent evaporation in a binary solvent system for controllable fabrication of porous fibers by electrospinning. *Thermal Science, 21(4),* 1821–1825. DOI 10.2298/TSCI160928074L.
28. Jalali, H., Abbassi, H. (2020). Analysis of the influence of viscosity and thermal conductivity on heat transfer by Al_2O_3-water nanofluid. *Fluid Dynamics & Materials Processing, 16(2),* 181–198. DOI 10.32604/fdmp.2020.07804.
29. Zhang, C., Wu, M. G. (2020). An analysis of the stretching mechanism of a liquid bridge in typical problems of dip-pen nanolithography by using computational fluid dynamics. *Fluid Dynamics & Materials Processing, 15(4),* 459–469. DOI 10.32604/fdmp.2019.08477.
30. Fan, J., Zhang, Y. R., Liu, Y., Wang, Y. H., Cao, F. Y. et al. (2019). Explanation of the cell orientation in a nanofiber membrane by the geometric potential theory. *Results in Physics, 15(11),* 102537. DOI 10.1016/j.rinp.2019.102537.
31. Yao, X., He, J. H. (2020). On fabrication of nanoscale non-smooth fibers with high geometric potential and nanoparticle's non-linear vibration. *Thermal Science, 24(4),* 2491–2497. DOI 10.2298/TSCI2004491Y.